In Silico Design and Analysis of Dengue Virus (DENV) Peptide Inhibitors

Chandreeka Thinakaran[1], Lai Thai Leong[1], & Sharleen Livina Isaac[2]

[1]Department of Cell & Molecular Biology, Faculty of Biotechnology and Biomolecular Sciences, Universiti Putra Malaysia (UPM), 43400 Serdang, Selangor, Malaysia.
[2]Department of Microbiology, Faculty of Biotechnology and Biomolecular Sciences, Universiti Putra Malaysia (UPM), 43400 Serdang, Selangor, Malaysia.

ABSTRACT

The dengue non-structural proteins, NS1, NS2B/NS3 and NS5 are key targets for antiviral design. In this study, peptide inhibitors were designed using different approaches against different viral proteins. For NS5, peptide inhibitor was designed based on the protein-protein interaction of DENV2 NS5 and signal transducer and activator of transcription 2 protein while alpha helix based peptide inhibitor was used to target the beta-roll region of NS1 to prevent NS1 from associating with lipid molecules to form NS1 hexamer. Targeting the NS2B/NS3, cyclic peptide was designed using scaffold engineering of sunflower trypsin inhibitor-1 (SFTI-1). Homology modelling of crystal structures was performed on proteins obtained from the Protein Data Bank. Subsequently, molecular docking was carried out to determine the candidate wild-type peptides before performing mutagenesis. Then, molecular docking was performed to determine the best mutant peptides. The results revealed that peptide 1T193F, peptide Magainin-II-A15R and SFT1-1-Capsid can be potential therapeutic peptides for dengue. Finally, the genetic circuit was designed to synthesise these antiviral peptides (output) identified using *Escherichia coli* as the chassis and glucose as the input.

1.0 INTRODUCTION

Dengue virus (DENV) is a positive stranded RNA virus belonging to the family of *Flaviviridae* together with Zika virus and Japan encephalitis virus. Its genome is 11 kb in size and translates into three structural proteins and seven non-structural (NS) proteins in the event of proteolytic processing. Transmitted by *Aedes* mosquitoes, DENV consists of four serotypes (DENV-1, DENV-2, DENV-3 and DENV-4) with each serotype able to cause a wide range of disease from mild to increasing severity (Chen & Vasilakis, 2011). The occurrence of dengue hemorrhagic fever and dengue shock syndrome have been a major cause of death among patients. With over 400 million infections occurring annually, dengue is currently endemic in over 100 countries (Bhatt et al., 2013). According to the World Health Organization (WHO), 70% of the disease burden lies within the Asian population. Although an influx of drugs and vaccine candidates are continually entering clinical trials, till date, none have passed the safety and efficacy tests (Lim, 2019; Torresi et al., 2017; Wilder Smith et al., 2010).

In this study, NS1, NS2B/NS3 and NS5 were selected as the target for drug design. NS1 dimer is formed when two monomers of the NS1 interlock with each other via disulphide linkage (Gonçalves et al., 2019). The region where monomer interlock is called the beta-roll. The beta roll is also called the hydrophobic core and gives the hydrophobic interface of the dimer (Watterson et al., 2016). This hydrophobic region of the NS1 dimer protein is important for associating with lipid molecules. When three dimer NS1 interact with the same lipid molecule, they form a hexamer structure. The hexamer structure of NS1 is responsible for the severe dengue diseases. Designing a drug that binds to the hydrophobic core, will prevent the protein from associating with lipid molecules and ultimately preventing secretion of this viral toxin out of the infected cell into the human blood plasma. Meanwhile, NS3 is a bi-domain protein, which consists of a protease domain and another domain of RNA helicase, nucleoside triphosphatase (NTPase) and 5' terminal RNA triphosphatase (RTPase) domain at the N- and C-termini respectively

(Shiryaev et al., 2007). In order for the proteolytic activity of NS3 to be fully executed, the binding with NS2B is essential. In contrast, NS5 is a dimeric protein consisting of an RNA-dependent RNA polymerase (RdRp) domain and a methyltransferase (MTase) domain at the N-terminal and C-terminal respectively (El Sahili et al., 2019). Peptides are well known for being cheap, highly specific, and highly cell-permeable (Gupta et al., 2013). In fact, peptide-based antivirals were shown to inhibit dengue protein, proving the feasibility of anti-dengue peptide design (Lin et al., 2017). Meanwhile, cyclic peptides have exceptional stability and high proteolytic resistance, making them particularly desirable to target proteases, e.g. DENV NS2B/NS3 (Colgrave & Craik, 2004; Craik,et al., 2018). Hence, peptide cyclisation was selected as the strategy to avoid their degradation by NS2B/NS3. This was achieved using scaffold engineering of sunflower trypsin inhibitor-1 (SFTI-1), where the prime and non-prime residues of SFTI-1 were substituted with polyprotein cleavage site sequences. STAT2 is an important protein-coding gene in the interferon (IFN) pathway that shields the body from acute viral infections and other inflammatory responses. However, DENV NS5 degrades STAT2 as an evasion strategy to mask itself from the host immune response (Ashour et al., 2009; Ashour et al., 2010). This then prevents the transcription of IFN- stimulated genes (ISGs) (Platanitis et al., 2019). So, a peptide inhibitor was designed based on the protein-protein interaction (PPI) of DENV2 NS5 and signal transducer and activator of transcription 2 (STAT2) protein.

To yield these peptides, one common approach is to use industrial fermentation for large-scale production. Cells are able to respond to different signals by activating different gene expression for environmental navigation, communication and building of complex patterns (Brophy and Voigt 2014). These properties are exploited using engineered organisms that are favoured for industrial fermentation due to their cost-saving milder manufacturing conditions, better sustainability of the chemical manufacture and biomass conversion to more profitable products (Keasling, 2010, Kim et. al., 2018). Nevertheless, the increased metabolic burden and metabolic imbalances can reduce the production efficiency (Kim et. al., 2018, Dahl et al., 2013; Lim et al., 2016). Synthetic biology was shown to benefit industrial production of materials using suitable genetic circuits, such as increased yield of desired compounds, separation of cell growth from heterologous gene expression and (Izard et. al., 2015, Chou & Keasling, 2013, Brockman & Prather, 2015; Gupta et al., 2017). Similar to the electric circuits, the genetic circuits biologically receive and compute the inputs and finally provide the output (Brophy & Voigt, 2014).

2.0 METHODOLOGY

2.1 Structural Retrieval

The crystal structures of DENV-2 NS5 (PDB ID: 5ZQK), Zika virus RdRp in complex with STAT2 (PDB ID: 6UX2), DENV-2 NS1 protein (PDB ID: 4O6B); alpha helix peptides crystal structures (PDB ID:4MGP), (PDB ID:1OB4), (PDB ID:1OB6), (PDB ID: 1OB7), DENV-2 NS2B/NS3 (PDB ID: 4M9K) and STFI-1 in complex with bovine trypsin (PDB ID: 1SFI) were obtained from RCSB Protein Data Bank. The crystal structure of bovine trypsin was subsequently removed from 1SFI. Crystal structures were visualized in UCSF Chimera v1.15 (Pettersen et al., 2004) to examine for missing residues.

2.2 Homology Modelling & Structure Validation

Homology modeling of NS5 protein was performed to fill in missing residues in all crystal structures using SWISS-Model web server (https://swissmodel.expasy.org/) while homology modeling of NS1 was performed through YASARA (Krieger & Vriend, 2014). The missing residues of NS2B/NS3 were performed using the BuildLoop and OptimizeLoop command of YASARA. Quality of the models were then assessed using ProCheck (Laskowski et al., 1993) and ERRAT (Colovos & Yeates, 1993) and VERIFY 3D (Bowie et al., 1991) from the SAVESv6.0 server (https://saves.mbi.ucla.edu/).

2.3 Determination of Interacting Residues

DENV-2 NS2B/NS3 and SFTI-1 docking was performed using HADDOCK web server (https://wenmr.science.uu.nl/haddock2.4/) to identify protein-peptide interaction sites. The default parameters were used. Since no active site inhibitor has been co-crystallised with DENV2 NS2B/NS3, literature search (Lin et al., 2016) and PDBSum were used to identify the DENV-3 NS2B/NS3 residues that interacts with aprotinin (PDB ID: 3U1J). The residues identified were then aligned with the DENV2 counterparts for selection as the active residues in HADDOCK, i.e. residues 80-86, 1029-1032, 1034-1036, 1051, 1072-1075, 1129-1135, 1150-1155 and 1161. Default setting was used in the docking except the specification of SFTI-1 as a cyclic peptide and the selection of previously reported residues 2-7 as the active residues (De Veer et al., 2016). Passive residues were automatically defined around the active sites. DENV-2 NS5 and STAT2 docking was performed using HADDOCK to identify protein-protein interaction sites. The default parameters were used. The active site residues/binding sites defined in the NS5 protein were P354-T362, Q754-L757 and E866-S878 while in STAT2 were F175, R176, Q200, L203, N204, D207, Q289, D291, P292 (Wang et al., 2020). Passive residues were automatically defined around the active sites. The candidate native peptides were chosen from the STAT2 protein domain based on the protein-protein interface. In contrast, the alpha helix peptides to be docked against the NS1 DENV-2 protein was obtained from the Collection of Microbial Peptides (Waghu et al., 2015). Molecular docking of alpha helix peptides and NS1 DENV-2 protein was performed using the VINA (Vina Is Not Autodock) docking program within YASARA (Yet Another Scientific Artificial Reality Application) (Trott & Olson, 2009). These peptides were docked against the beta-roll region (1-29 amino acid residue) of the NS1 protein. HADDOCK web server was used to validate the accuracy of the docking. LigPlot+ (Wallace et al., 1995) was used to visualize the interacting complexes.

2.4 Peptide Design via Mutagenesis

For the DENV-2 NS1 protein, the alpha helix peptide with highest positive binding energy (Kcal/mol) and smallest dissociation constant (Kd) was used as a benchmark to produce mutants with better binding energy and dissociation constant. The site-directed saturated mutagenesis was performed using the FoldX force field within YASARA software. The mutagenesis was done while the native peptide was still bound to the beta-roll of the DENV-2 NS1 protein. The mutants that were produced were optimized using the ‘RepairPDB’ function within the FoldX. For DENV-2 NS2B/NS3, multiple sequence alignment was conducted using DENV1 strain Hawaii (GenBank accession no. KM204119), DENV2 strain 16681 (GenBank accession no. U87411) and strain New Guinea C (NGC) (GenBank accession no. M29095), DENV3 strain H87 (GenBank accession no. M93130), DENV4 strain H241 (GenBank accession no. AY947539), Yellow Fever virus (YFV) Abisi strain (GenBank accession no. AY640589), Zika virus (ZIKV) Malaysia/1966 strain P6–740 (GenBank accession no. KX377336), West Nile virus (WNV) Uganda strain (B956) (GenBank accession no. AY532665) to derive the cleavage site sequences of DENV2 strain 16681 and strain NGC. All prime and non-prime side residues were substituted with the amino acid sequences derived from the proteolytic cleavage site (Supplementary Table S5) except P3 residues, Cys-3 due to the importance of this residue in stabilising disulphide bridge formation. Mutagenesis was performed using YASARA, followed by minimisation which gives the value of final energy (Supplementary Table S5). In DENV-2 NS5 study, computational saturation mutagenesis using Mutatex with Python wrapper function (https://github.com/ELELAB/mutatex) employing FoldX (Guerois et al., 2002) was used to mutate different amino acids of each position of the wild type antiviral peptide sequence. Quick optimization of native structures were performed using the ‘RepairPDB’ function within FoldX and the ‘AnalyseComplex’ to compute Gibbs’ energy of proteins- peptide complexes.

2.4 Molecular Docking

For DENV-2 NS1, the binding energy of mutant peptides was analysed using the local docking method of YASARA. The HADDOCK score was also analysed for the both mutant peptide-NS1 protein complexes and native peptide-NS1 protein complexes (. Molecular docking of NS5 and NS2B/NS3 proteins and their respective peptides were performed through the HADDOCK web server using the default parameters, except the specification of SFTI-1 mutants as a cyclic peptide and the selection of residues 2-7 as the active residues of Molecule 2 for the latter. For DENV2 NS5, both candidate wildtype and mutant peptides were docked with the DENV2 NS5 protein through the using the default parameters. The active residues of mutant peptides were defined based on the direct interaction of wildtype residues. The passive residues were automatically defined around the active sites. Pymol (The PyMOL Molecular Graphics System, Version 2.0 Schrodinger, LLC) and LigPlot+ were used to visualize the interacting residues.

2.5 Genetic Circuit Design

The chassis for the genetic circuit design was determined to be *Escherichia coli* based on the criteria of simplicity, scalability, low cost of maintenance and intensive studies in its physiology and metabolism. The input and output of the genetic device was set to be glucose and antiviral peptides respectively. The genetic components of the systems were then selected based on the search and comparison of the suitable Biobricks from SynBioHub (https://synbiohub.org/) and the iGEM Registry of Standard Biological Parts (http://parts.igem.org/). Suitable modules and logic gates were selected based on the process intended. Biobricks that confer the properties of logical functions were chosen to optimise the genetic circuit. The information on cell burden, whenever available, was considered in the selection of Biobricks. The genetic circuit design was illustrated with the synthetic biology open language (SBOL) 3.0 using SBOLCanvas (https://sbolcanvas.org/canvas/).

3.0 RESULTS & DISCUSSION

3.1 Homology Modelling & Structure Validation

All protein crystal structures obtained from the PDB contained missing residues. Missing residue often reduces the accuracy during molecular docking. Hence, homology modelling was performed on the crystal structures.

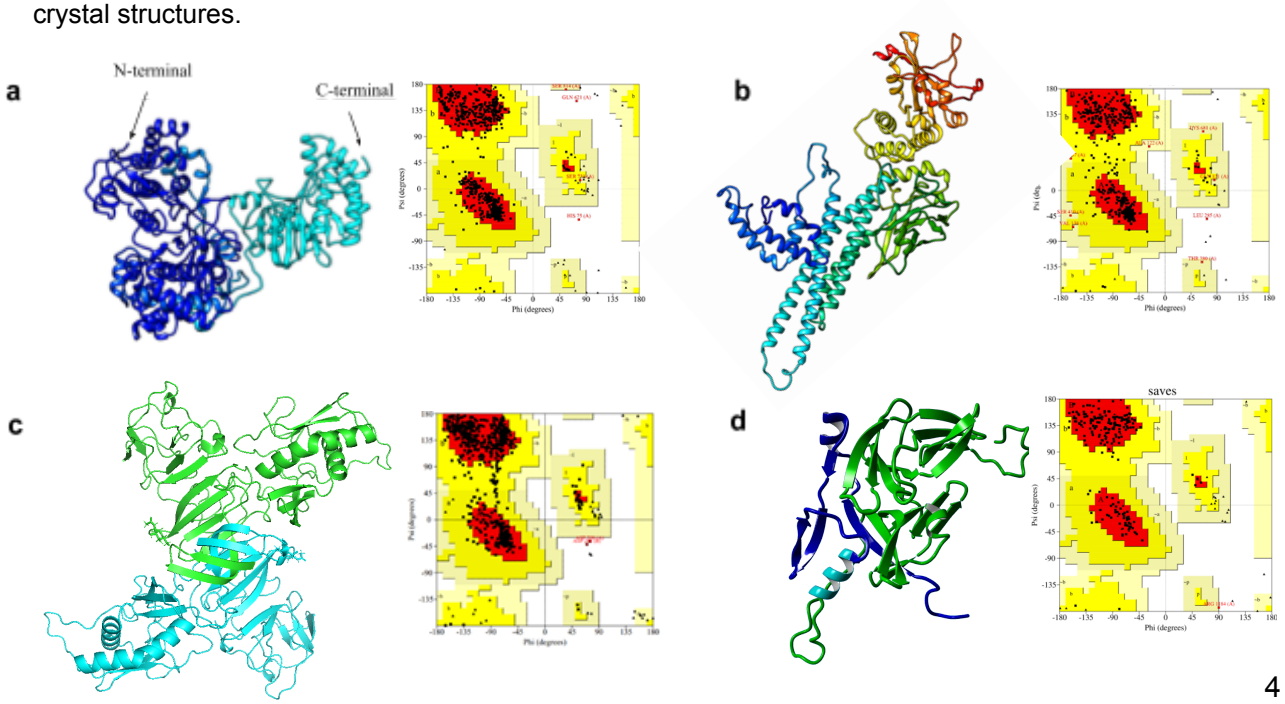

Figure 1. Homology models of proteins in ribbon representation and Ramachandran plot generated from PROCHECK. **(a)** DENV-2 NS5 protein. **(b)** STAT2 protein. **(c)** NS1 protein. **(d)** NS2B-NS3 protein.

From the Ramachandran plot of DENV NS5 in Figure 1. a, 94.3% of protein residues were in the favored region, 5.2% in the additional allowed region, 0.3% in the generously allowed region and 0.3% in the disallowed region while in STAT2 (Figure 1. b), 90.8% of protein residues were in the favored region, 7.9% in the additional allowed region, 1.1% in the generously allowed region and 0.2% in the disallowed region. The Ramachandran plot analysis for NS1 protein (Figure 1. c) showed that 87.2% of the amino acid residues was in the favored region, 12.5% in additional allowed regions, 0.0% in generously allowed regions and 0.3% in disallowed regions. For DENV NS2B/NS3, 91.9% of the amino acid residues was in the favored region, 7.6% in additional allowed regions, 0.0% in generously allowed regions and 0.5% in disallowed regions based on the Ramachandran plot analysis. According to the Ramachandran analysis, a benchmark for a good quality model, 90% of residues are found in the favored region. Therefore, all models generated were good quality models. The ERRAT quality factor scores for the proteins were NS1;92.868, NS5;94.220, STAT2;94.1718 and NS2B/NS3;76.1702 (Supplementary Figure S2). The VERIFY 3D analysis showed that NS1;82.24% of the residues had averaged 3D-1D score >= 0.2 – Passed (Supplementary Figure S1).

3.2 Determination of interacting residues

Based on the protein-protein interaction after DENV-2 NS5 and STAT2 docking (Figure 2. a), only two residues from the DENV2 NS5 Mtase domain were involved in the interaction while three fourth of the interacting residues were from the RdRp domain. Likewise, two residues were from the N-terminal domain (ND; a.a 1-136) of STAT2 while the rest were from the coiled-coil domain (CCD; a.a 137-316). From the interaction sites, candidate wildtype peptides were chosen from the STAT2 CCD domain.

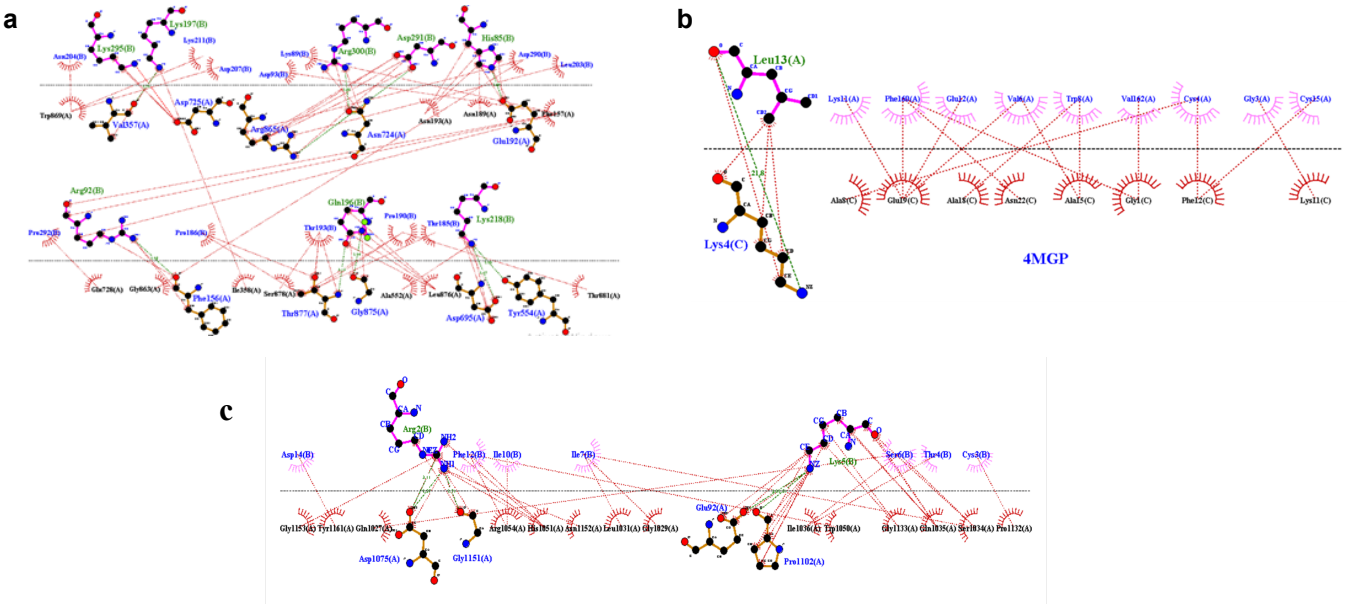

Figure 2. 2D visualization of complexes using the DIMPLOT tool in LigPlot+. Dotted green lines and red lines indicate hydrogen bond interaction and hydrophobic interactions, respectively**. a.** DENV-2 NS5-STAT2 complex. **b.** NS1-4MGP complex **c.** DENV NS2B/NS3-SFTI-1 complex.

The residues involved in the DENV-2 NS2B/NS3 interaction with active site ligand was predicted based on the comparison with DENV-3 NS2B/NS3, 3U1J and previous report (Lin et al., 2016). According to Figure 2c, nine out of 14 residues of the wild-type SFTI-1 were shown to be involved in non-covalent interactions with the NS2B/NS3, showing its ability to form strong interactions with this target protein. The P3' and P4' residues, corresponding to the residues 8 and 9 are not involved in any interaction with the target protein, which may either due to the artifact caused by manual selection residues 2 to 9 as the active residues during docking using the HADDOCK or its negligible role in binding with the NS2B/NS3 (De Veer et al., 2016). Only two of the catalytic triad, i.e. H1951 and A1075 were involved in the interaction with wild-type SFTI-1, showing that mutagenesis and optimisation of SFTI-1 which enables its interaction with serine can improve its binding activity.

In docking studies of DENV-2 NS1, the peptide with PDB ID 4MGP showed high positive binding energy of +9.52 kcal/mol towards the beta-roll of NS1 protein compared to the other 3 alpha-helix peptides (Table 1). The dissociation constant of 4MGP was extremely small; 105669 pM, compared to the other peptides. Lower dissociation constant indicates higher binding affinity of peptide towards a protein. Therefore, peptide 4MGP was selected for further analysis. It was found that there was one hydrogen bonding between residue O Leu13 of NS1 and NZ Lys4 of 4MGP (Supplementary Table S2).

Table 1:Molecular docking analysis obtained from YASARA of 4 native alpha helix peptides

PDB ID	Binding energy (Kcal/mol)	Dissociation constant (pM)
4MGP	9.52	105669
1OB4	9.27	159784
1OB6	12.96	317.975
1OB7	9.22	173854

3.3 Mutagenesis Analysis

For NS5-peptide complexes, the binding energy difference after mutation (ΔΔG) and the interaction energy are illustrated in a heatmap in Figure 3. Few mutant amino acid residues had better stability and interaction compared to the wildtype.

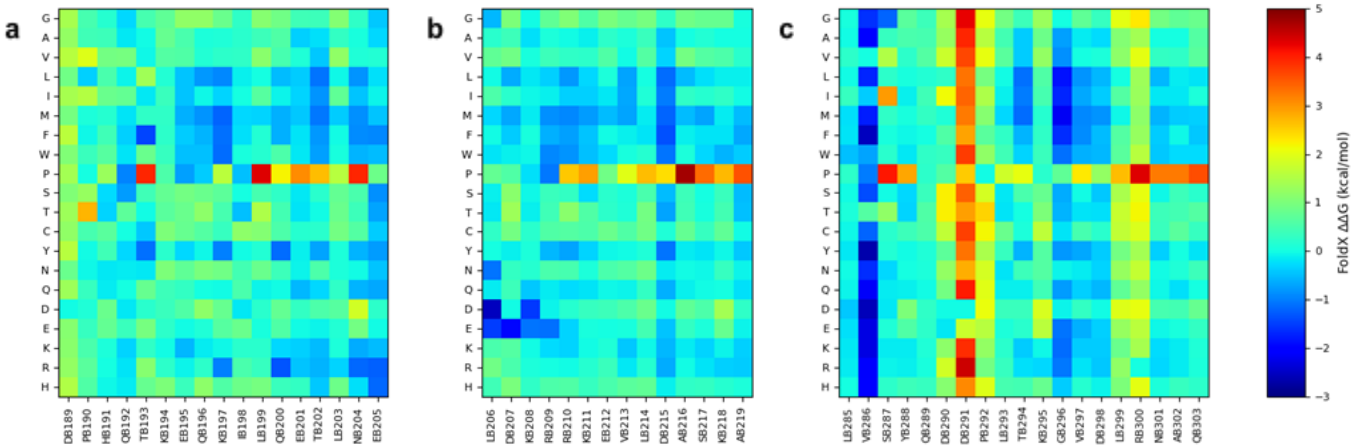

Figure 3. In silico mutational scan of DENV-2 NS5- wildtype peptides using the empirical energy function FoldX. The average ΔΔG is shown in a heatmap with a corresponding color gradient at each point of mutation. **a.** Peptide 1 (residues D189-E205). **b.** Peptide 2 (residues L206-A219). **c.** Peptide 3 (residues L285-Q303).

A more negative ΔΔG value indicates more stability than a positive ΔΔG value. The amino acid substitution with a higher positive ΔΔG value had a destabilizing effect. Interestingly, DB189, DB291, LB299 and RB300 were indispensable in the interaction. This is largely due to the important function of the residue in preserving its integrity of structure and binding interface between DENV2 NS5 and peptide. However, T193F, K197M, Q200R, E205R, L206D, D207E, K208D, D215F, V286Y, V286D, V286F, G296M mutants were considered for further analysis because they were more stable than the wildtype residues. In the NS1 mutagenesis study, the alpha helix peptide 4MGP was selected for site-directed saturated mutagenesis. 10 mutants, i.e. Gly1Lys, Gly1Gln, Gly1Arg, Ala15Glu, Ala15Gln, Ala15Lys, Ala15Arg, Glu19Lys, Glu19Arg, and Asn22Lys, were produced (Supplementary Table S1). The ΔΔG between the interacting molecules of DENV-2 NS1-mutant peptide complex and DENV-2 NS1-wildtype 4MGP peptide complex were studied. All 10 mutants created, displayed negative ΔΔG, while the wildtype-4MGP showed positive ΔΔG. Negative binding energy of the mutant peptide indicated that the mutants had better binding stability toward the NS1 protein compared to the wildtype 4MGP peptide. The site-directed saturated mutagenesis produced mutants with improved binding stability than the wildtype peptide. Since different sequences of the polyprotein cleavage sites already exist naturally, these sequences are used for direct substitution of prime and non-prime side residues of the SFTI-1 for mutagenesis. This mimics the natural substrates of the NS2B/NS3 with the aim of blocking its proteolytic activity via competitive inhibition. Besides, these sequences are essential for the NS2B/NS3 recognition in dengue life cycle and hence it may be unlikely that escape mutations would occur, causing the NS2B/NS3 to lose its ability to recognise its natural substrates. The final energy after minimisation showed SFTI-1-capsid to have the highest stability, showing its suitability as a promising NS2B/NS3 inhibitor. In the future, saturation mutagenesis of the best binder, i.e. SFTI-1-capsid obtained in this study can be conducted to investigate the effect of increased hydrophobicity on its potency, e.g. binding energy. Due to the high charge of the polar prime (P) side residues, the incorporation of non-polar residues can offset the P side polarity, thereby rendering the SFTI-1 mutants more cell-permeable (Lin et al., 2017).

3.4 Molecular Docking

The result of molecular docking between DENV-2 NS5 and mutant peptides revealed that most mutant peptides showed better HADDOCK score (the more negative the better) than the wild peptides (Supplementary Table S3). However, mutant peptide 1T193F with sequence DPHQFKEQKILQETLNE showed the lowest and best HADDOCK score of -59.4 +/6.7 compared to the rest of the mutant peptides. In Figure 4. a, the docked DENV-2 NS5-1T193F peptide complex formed two hydrogen bonds; E205 with K128 and G129 respectively and 15 hydrophobic bonds.

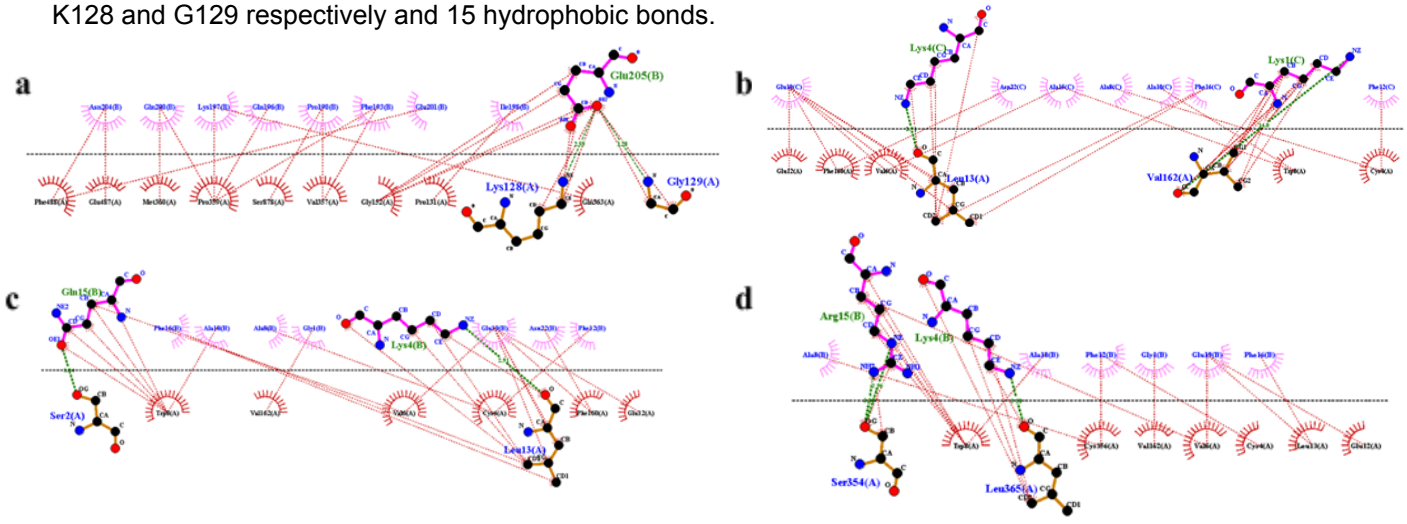

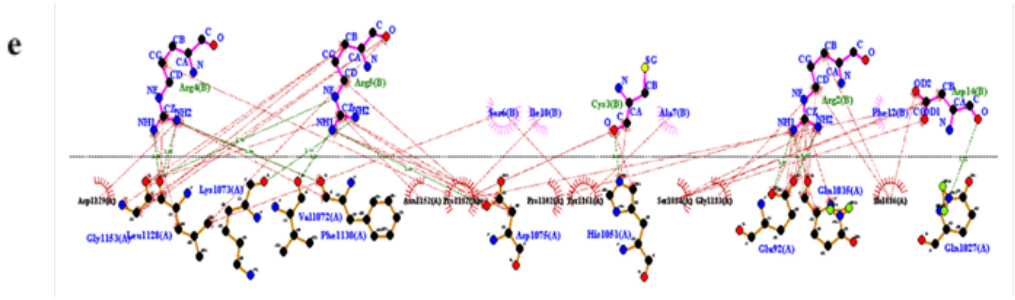

Figure 4. Interacting residues visualized through LigPlot+. Dotted green lines and red lines indicate hydrogen bond interaction and hydrophobic interactions, respectively. **a.** DENV-2 NS5- peptide 1T193F complex. **b.** DENV-2 NS1- peptide 4MGP Gly1Lys complex. **c.** DENV NS1- peptide 4MGP Ala15Gln complex. **d.** DENV-2 NS1-peptide 4MGP Ala15Arg complex. **e.** NS2B/NS3-SFTI-1-capsid complex.

The additional hydrophobic bonds formed between DENV-2 NS5 and peptide 1T193F compared to the wildtype shows the possibility of the mutant peptide 1T193F to competitively bind to NS5 viral protein.

The binding energy of the top three mutant peptides; Gly1Lys, Ala15Gln and Ala15Arg were studied. The mutants had high binding energies of 11.29 kcal/mol, 11.71Kcal/mol and 11.95 kcal/mol respectively while the dissociation constant was 5327.449 pM, 2595.716 pM, 1751.725 pM respectively (Supplementary Table S2). Two hydrogen bonds were formed between the mutant peptide Gly1Lys-NS1 protein and mutant peptide Ala15Gln-NS1 protein. Three hydrogen bonds formed between Ala15Arg-NS1 protein (Supplementary Table S2). Additional hydrogen bonds formed compared to the ones formed between native peptide 4MGP-NS1 protein. The top three mutants; Gly1Lys, Ala15Gln and Ala15Arg were docked again using HADDOCK for further validation of docking accuracy. The HADDOCK score analysis showed (Supplementary Table S4) that the native peptide scored -67.5 +/- 1.4, Gly1Lys scored -69.1 +/- 2.7, Ala15Arg scored -65.7 +/- 9.7 and Ala15Gln scored -65.6 +/- 5.1. Although Gly1Lys and Ala15Gln recorded lower docking score than native peptide, the margin of error for both of the mutants is larger compared to the native peptide indicating that they are having better HADDOCK score compared to the native peptide.

On the other hand, based on the HADDOCK binding energy, it was clear that the SFTI-1-capsid is the best NS2B/NS3 inhibitor with the value of -211.773 kcal/mol as compared to the second best binder, SFTI-1-3-4A (-166.8 kcal/mol) and wild-type SFTI-1 (-162.161 kcal/mol). Using isothermal titration calorimetry, Lin et al. (2017) reported entropy to be the sole contributing factor to the binding of peptide inhibitors to NS2B/NS3 at its active site. Since a more desolvation energy results increases the entropy, the lowest desolvation energy of SFTI-1-capsid probably explains its underlying reason of getting the best docking result. Despite having worse results for other properties, e.g. van der Waals energy, electrostatic energy and restraints violation energy, they can be interpreted to have less significant effect on NS2B/NS3-peptide binding although an increase in hydrogen bonding is correlated with improvements in binding affinity (Lin et al., 2017). Similar aprotinin-based inhibitor based capsid sequence was also showed to be one of the only three cleavage sequences with three hydrogen bonding between the main and side chains of P1 and with DENV-3 NS2B/NSOnly two of the catalytic triad, i.e. H1951 and A1075 were involved in the interaction with wild-type SFTI-1, showing that mutagenesis and optimisation of SFTI-1 which enables its interaction with serine can improve its binding activity. 3 more than 50% of the time in molecular dynamics simulations, a desirable property which probably exists in DENV-2 NS2B/NS3-STFI-1-capsid interaction as well. The SFTI-1 mutant entropy can be increased via enhanced rigidity through incorporation of hydrophobic residues, making it more potent (Lin et al., 2017). According to Figure 4e, nine out of 14 residues of the SFTI-1-capsid was shown to involve in non-covalent

interactions with the NS2B/NS3 but with a greater number of hydrogen bonding and hydrophobic interactions, showing its possibility of having higher activity as compared to the wild-type SFTI-1. Surprisingly, the residues 8 and 9 were not interacting with the NS2B/NS3, probably explaining the reason why these two sites were not targeted for substitution of previous design of STFI-1-based inhibitors against other proteases, which otherwise may indicates the artifact caused by manual selection residues 2 to 9 as the active residues during docking using the HADDOCK (De Veer et al., 2016). Similarly, only H1951 and A1075 of NS2B/NS3 were involved in the interaction with SFTI-1-capsid, probably indicating the future space of peptide sequence optimization to interact with this residue. As compared to T4 in wild-type SFTI-1, K4 in SFTI-1-capsid is able to have more interactions, i.e. three hydrogen bonds with Leu1128 and F1130 and eight hydrophobic interactions with L1128, D1129, F1130 and N1152. This clearly reflects the preference of NS2B/NS3 for basic residue at this P2 side. The number of hydrogen bonds between this mutant peptide and NS2B/NS3 is also more than the wild-type one, i.e. twelve bonds.

3.5 Genetic Circuit Design

In the genetic circuit design (Figure 5), *Escherichia coli* was chosen as the chassis since it is simple in addition to being well studied physiologically and genetically. Glucose is the main carbon source of the chassis for peptide biosynthesis due to its low cost and large supply, ensuring the scalability of the design in industrial applications. For peptide yield maximisation, the carbon flux needs to be directed in favour of its biosynthesis (Kim et. al., 2018). Cell growth control channels the nutrients for antiviral peptide synthesis instead of unwanted biomass production. Conventionally, cell growth control using antibiotics kills the chassis while essential nutrient limitation affects the yield of peptides due to its high demand for carbon and nitrogen. For genetic circuit optimization, the knockout strain of *E. coli* was used in which it is unable to produce its own β and β' subunits of the RNA polymerase. Under the control of pLux promoter, the chassis can only grow upon the addition of N-3-oxohexanoyl-L-homoserine lactone (HSL), which binds with the constitutively expressed LuxR regulator for expression of *rpoB* and *rpoC* genes, the genes of the two RNA polymerase subunits aforementioned. HSL removal upon reaching the desired population stops the chassis from growing but retains active metabolism for peptide synthesis. Izard et. al. (2015) showed a twofold increase in glycerol production without killing the cells using controlled expression of RNA polymerase.

The design shown in this study (Figure 5) separates the growth of chassis from the production phase of peptide synthesis to prevent growth-inhibitory carbon flux reduction that can ultimately result in low peptide synthesis (Min et al., 2017; Noh et al., 2017). In the production phase, the presence of IPTG induces T7 RNA polymerase and cI repressor expression, both of which are placed under the tight control of pLacIQ and Lac-UV5 promoter. The pLacIQ is stronger than the wild-type pLacI promoter, thereby producing more repressors which reduces the leakiness of downstream expression. Meanwhile, Lac-UV is independent of catabolite repression by glucose, enabling T7 polymerase and cI expression under high concentration of glucose, the main carbon source of fermentation. During fermentation, no further cell growth is intended. The cI repressor strengthens the cell growth control by binding with the cI operator upstream of the *rpoB* and *rpoC* genes to block any possible leaky expression.

With T7 RNA polymerase production, antiviral peptides under the control *T7* promoter can be expressed. Peptide overexpression forms inclusion bodies, causing cell stress and cytotoxicity. Hence, a stress-inducible TetR expression system was incorporated. Making use of the sensitivity of *pIbpAB* promoter to the presence of inclusion bodies, this activates the expression of TetR repressor. The TetR repressors bind to the *TetO* operator upstream of the peptide gene, thereby inhibiting further overexpression of peptides and cytotoxic inclusion bodies accumulation. Besides, the arabinose-inducible system was included where the holin and endolysin are only expressed after fulfilling two conditions, the

absence of glucose and presence of arabinose. The high glucose concentration and absence of arabinose prevent unintended holin and endolysin expression by repressing the P_{BAD} promoter during the production phase of fermentation. In contrast, glucose deprivation and presence of arabinose at the final phase of fermentation activate holin and endolysin expression that kills the chassis and releases the peptide products simultaneously, enabling the DENV peptide inhibitors to be harvested. No antitoxin, specifically antiholin, is included in the genetic circuit to prevent the emergence of escape phenotypes among possible mutants due to constitutive expression of antitoxin. The P_{BAD} promoter was chosen due to its low cost and non-toxicity of L-arabinose as the inducer, low metabolic burden, high level of heterologous expression and tight transcriptional regulation (Széliová et al., 2016). The control of via glucose deprivation and arabinose induction also takes the initiation of cell lysis to hand.

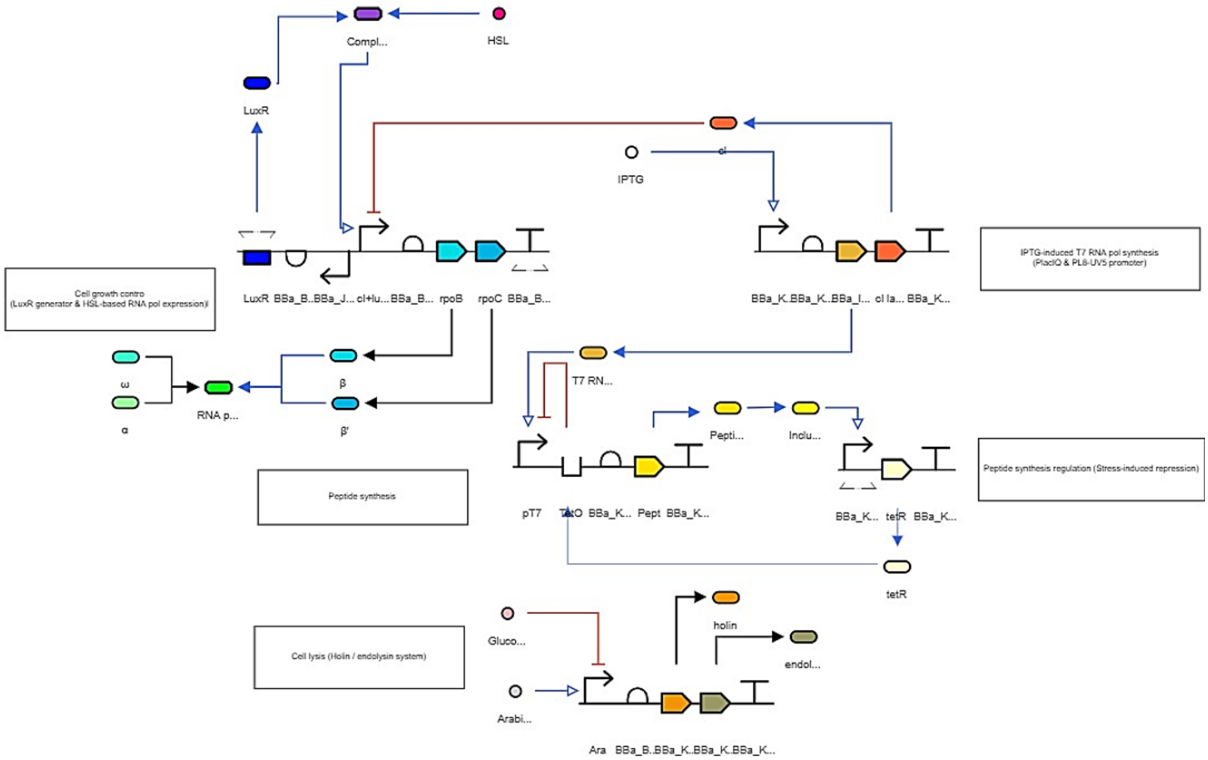

Figure 5. The design of the genetic circuit shown in SBOL 3.0

4.0 CONCLUSION

Despite many long-term researches have been conducted conventionally in search of prophylaxis or treatment, many diseases, including dengue remain an unsolved challenge to human health. Venture into emerging fields like synthetic biology, promises new approaches to address such yet unsolvable challenges. Our in silico analysis showed the potential of using synthetic peptides as dengue treatment. Peptide Magainin-II-A15R (GIGKFLHAAKKFAKRFVAEIMNS), SFT1-1-Capsid (GRCRRSAGMICFPD) and 1T193F (DPHQFKEQKILQETLNE) were shown to be the best inhibitor against NS5, NS1 and NS2B/NS3 via its blockage of the pathogenic NS1 hexamerisation, NS5-disrupting and antiproteolytic activities respectively. However, molecular dynamic simulation and wet lab analysis should be conducted in the future to validate the accuracy of the in silico analysis performed in this study. The genetic circuit incorporated the HSL-based cell growth control as well as IPTG-induced expression of T7 RNA polymerase and CI repressor to optimise the carbon flux, peptide expression and its regulation by the T7

RNA polymerase and Tet repressor, cell stress-induced expression of Tet repressor to prevent cytotoxic inclusion bodies accumulation and arabinose-inducible activation of holin-endolysin system for cell lysis, thereby killing the chassis and release the peptide products simultaneously at the final stage of fermentation.

REFERENCES

1. Ashour, J., Laurent-Rolle, M., Shi, P. Y., & García-Sastre, A. (2009). NS5 of dengue virus mediates STAT2 binding and degradation. *Journal of virology*, *83*(11), 5408-5418.
2. Ashour, J., Morrison, J., Laurent-Rolle, M., Belicha-Villanueva, A., Plumlee, C. R., Bernal-Rubio, D., ... & García-Sastre, A. (2010). Mouse STAT2 restricts early dengue virus replication. *Cell host & microbe*, *8*(5), 410-421.
3. Bhatt, S., Gething, P. W., Brady, O. J., Messina, J. P., Farlow, A. W., Moyes, C. L., ... & Hay, S. I. (2013). The global distribution and burden of dengue. *Nature*, *496*(7446), 504-507.
4. Brockman, I. M., & Prather, K. L. (2015). Dynamic knockdown of E. coli central metabolism for redirecting fluxes of primary metabolites. *Metabolic engineering, 28*, 104-113.
5. Brophy, J. A., & Voigt, C. A. (2014). Principles of genetic circuit design. *Nature methods, 11*(5), 508-520.
6. Chen, R., & Vasilakis, N. (2011). Dengue—quo tu et quo vadis?. *Viruses*, *3*(9), 1562-1608.
7. Chou, H. H., & Keasling, J. D. (2013). Programming adaptive control to evolve increased metabolite production. *Nature communications, 4*(1), 1-8.
8. Colgrave, M. L., & Craik, D. J. (2004). Thermal, chemical, and enzymatic stability of the cyclotide kalata B1: the importance of the cyclic cystine knot. *Biochemistry, 43*(20), 5965–5975. https://doi.org/10.1021/bi049711q
9. Colovos, C., & Yeates, T. O. (1993). Verification of protein structures: patterns of nonbonded atomic interactions. *Protein science*, *2*(9), 1511-1519.
10. Craik, D. J., Lee, M. H., Rehm, F., Tombling, B., Doffek, B., & Peacock, H. (2018). Ribosomally-synthesised cyclic peptides from plants as drug leads and pharmaceutical scaffolds. *Bioorganic & Medicinal Chemistry*, *26*(10), 2727–2737. https://doi.org/10.1016/j.bmc.2017.08.005
11. Dahl, R. H., Zhang, F., Alonso-Gutierrez, J., Baidoo, E., Batth, T. S., Redding-Johanson, A. M., ... & Keasling, J. D. (2013). Engineering dynamic pathway regulation using stress-response promoters. *Nature biotechnology, 31*(11), 1039-1046.
12. De Veer, S. J., Swedberg, J. E., Brattsand, M., Clements, J. A., & Harris, J. M. (2016). Exploring the active site binding specificity of kallikrein-related peptidase 5 (KLK5) guides the design of new peptide substrates and inhibitors. Biological chemistry, 397(12), 1237-1249.
13. El Sahili, A., Soh, T. S., Schiltz, J., Gharbi-Ayachi, A., Seh, C. C., Shi, P. Y., ... & Lescar, J. (2019). NS5 from dengue virus serotype 2 can adopt a conformation analogous to that of its Zika virus and Japanese encephalitis virus homologues. *Journal of virology*, *94*(1), e01294-19.
14. Gonçalves, R. L., de Lima Menezes, G., Sussuchi, L., Moreli, M. L., Mottin, M., Andrade, C. H., Pereira, M., & da Silva, R. A. (2019). Dynamic behavior of Dengue and Zika viruses NS1 protein reveals monomer–monomer interaction mechanisms and insights to rational drug design. *Journal of Biomolecular Structure and Dynamics*, *38*(14), 4353–4363. https://doi.org/10.1080/07391102.2019.1677504
15. Guerois, R., Nielsen, J. E., & Serrano, L. (2002). Predicting changes in the stability of proteins and protein complexes: a study of more than 1000 mutations. *Journal of molecular biology*, *320*(2), 369-387.
16. Gupta, S., Kapoor, P., Chaudhary, K., Gautam, A., Kumar, R., Open Source Drug Discovery Consortium, & Raghava, G. P. (2013). In silico approach for predicting toxicity of peptides and proteins. *PloS one*, *8*(9), e73957.

17. Gupta, A., Reizman, I. M. B., Reisch, C. R., & Prather, K. L. (2017). Dynamic regulation of metabolic flux in engineered bacteria using a pathway-independent quorum-sensing circuit. *Nature biotechnology, 35*(3), 273-279.
18. Izard, J., Gomez Balderas, C. D., Ropers, D., Lacour, S., Song, X., Yang, Y., ... & de Jong, H. (2015). A synthetic growth switch based on controlled expression of RNA polymerase. *Molecular systems biology*, *11*(11), 840.
19. Keasling, J. D. (2010). Manufacturing molecules through metabolic engineering. *Science, 330*(6009), 1355-1358.
20. Kim, S. G., Noh, M. H., Lim, H. G., Jang, S., Jang, S., Koffas, M. A., & Jung, G. Y. (2018). Molecular parts and genetic circuits for metabolic engineering of microorganisms. *FEMS microbiology letters*, *365*(17), fny187.
21. Krieger, E., & Vriend, G. (2014). YASARA View—molecular graphics for all devices—from smartphones to workstations. *Bioinformatics*, *30*(20), 2981-2982.
22. Laskowski, R. A., MacArthur, M. W., Moss, D. S., & Thornton, J. M. (1993). PROCHECK: a program to check the stereochemical quality of protein structures. *Journal of applied crystallography*, *26*(2), 283-291.
23. Lim, S. P. (2019). Dengue drug discovery: Progress, challenges and outlook. *Antiviral research*, *163*, 156-178.
24. Lim, H. G., Noh, M. H., Jeong, J. H., Park, S., & Jung, G. Y. (2016). Optimum rebalancing of the 3-hydroxypropionic acid production pathway from glycerol in *Escherichia coli. ACS synthetic biology, 5*(11), 1247-1255.
25. Lin, K. H., Ali, A., Rusere, L., Soumana, D. I., Kurt Yilmaz, N., & Schiffer, C. A. (2017). Dengue virus NS2B/NS3 protease inhibitors exploiting the prime side. *Journal of virology, 91*(10), e00045-17.
26. Lin, K. H., Nalivaika, E. A., Prachanronarong, K. L., Yilmaz, N. K., & Schiffer, C. A. (2016). Dengue protease substrate recognition: binding of the prime side. *ACS infectious diseases*, *2*(10), 734-743.
27. Min, B. E., Hwang, H. G., Lim, H. G., & Jung, G. Y. (2017). Optimization of industrial microorganisms: recent advances in synthetic dynamic regulators. Journal of Industrial *Microbiology and Biotechnology, 44*(1), 89-98.
28. Pettersen, E. F., Goddard, T. D., Huang, C. C., Couch, G. S., Greenblatt, D. M., Meng, E. C., & Ferrin, T. E. (2004). UCSF Chimera—a visualization system for exploratory research and analysis. *Journal of computational chemistry*, 25(13), 1605-1612.
29. Platanitis, E., Demiroz, D., Schneller, A., Fischer, K., Capelle, C., Hartl, M., ... & Decker, T. (2019). A molecular switch from STAT2-IRF9 to ISGF3 underlies interferon-induced gene transcription. *Nature communications*, *10*(1), 1-17.
30. Széliová, D., Krahulec, J., Šafránek, M., Lišková, V., & Turňa, J. (2016). Modulation of heterologous expression from P_{BAD} promoter in *Escherichia coli* production strains. *Journal of biotechnology*, *236*, 1-9.
31. Torresi, J., Ebert, G., & Pellegrini, M. (2017). Vaccines licensed and in clinical trials for the prevention of dengue. *Human vaccines & immunotherapeutics*, *13*(5), 1059-1072.
32. Wallace, A. C., Laskowski, R. A., & Thornton, J. M. (1995). LIGPLOT: a program to generate schematic diagrams of protein-ligand interactions. *Protein engineering, design and selection*, *8*(2), 127-134.
33. Wang, B., Thurmond, S., Zhou, K., Sánchez-Aparicio, M. T., Fang, J., Lu, J., ... & Song, J. (2020). Structural basis for STAT2 suppression by flavivirus NS5. *Nature structural & molecular biology*, *27*(10), 875-885.

34. Watterson, D., Modhiran, N., & Young, P. R. (2016). The many faces of the flavivirus NS1 protein offer a multitude of options for inhibitor design. *Antiviral Research*, *130*, 7–18. https://doi.org/10.1016/j.antiviral.2016.02.014
35. Wilder-Smith, A., Ooi, E. E., Vasudevan, S. G., & Gubler, D. J. (2010). Update on dengue: epidemiology, virus evolution, antiviral drugs, and vaccine development. *Current infectious disease reports*, *12*(3), 157-164.
36. World Health Organization (WHO). (2012). Global strategy for dengue prevention and control 2012–2020. *WHO Library Cataloguing-in-Publication Data, Switzerland*.